Online State of Health Diagnostic Method of Battery cells in a Reconfigurable Battery System or Multilevel Inverter

Ali Mashayekh
Universität der Bundeswehr München

Mahdiye Khorasani
Universität der Bundeswehr München

Julian Estaller
Universität der Bundeswehr München

Johannes Buberger
Universität der Bundeswehr München

Online State of Health Diagnostic Method of Battery cells in a Reconfigurable Battery System or Multilevel Inverter

Ali Mashayekh[1], Mahdiye Khorasani[1], Julian Estaller[1], Johannes Buberger[1], Manuel Kuder[1,2], Richard Eckerle[1], Thomas Weyh[1]

[1] Universität der Bundeswehr München , Germany
[2] BAVERTIS GmbH, Neubiberg, Germany

Corresponding author: Ali Mashayekh, ali.mashayekh@unibw.de

Abstract

This study shows a novel online approach for characterizing battery cells or modules in any type of reconfigurable battery system (RBS) for electric driving applications, which allows neighboring cells or modules to switch in parallel. Also, the different representations (time and frequency domain) of conventional battery modeling based on equivalent circuit models (ECM) are described. Finally, it is shown that the balancing current of neighboring cells can be used to characterize the batteries' dynamic parameters and, as a result, estimate the state of health (SoH) and remaining useful life (RUL) of each cell individually.

1 Introduction

The demand for dependable electrified means of transportation based on electrical energy storage systems, above all battery systems, has been emerging with the goal of reducing local carbon emission [1]. Therefore, the improvement of characteristics of this system like reliability, effective driving range and lifetime has to be taken into consideration to be a valid substitution for conventional method of transportation [2]–[4]. Above all mentioned aspects, the lifetime of a battery electric vehicle (BEV) could be considered as a major drawback as opposed to conventional vehicles. Firstly, the system degradation is governed by a vast number of controllable and uncontrollable parameters like the charging/ discharging method and calendar aging of battery cells respectively. Secondly, it is difficult to accurately estimate the RUL and SoH due to the high number of interrelated and interdependent parameters. Battery degradation can be investigated with respect to electrochemical phenomena. In other words, it is stated as a decrease in effective nominal capacity or an increase in internal resistance. Battery aging is a complex phenomenon that is mostly caused by loss of conductivity, charge-transfer and double layer capacitance, solid electrolyte interface (SEI) formation, diffusion and lithium-plating [5]–[8].

Offline non-destructive characterization methods like electrochemical impedance spectroscopy (EIS) are used to deeply investigate the degradation of Lithium-ion (Li-Ion) battery cells. This approach is based on applying a sinusoidal perturbation signal (current, voltage) with a constant AC amplitude and the desired frequency range, and then measuring the amplitude and phase shift of the feedback signal (voltage, current) of the system [8]–[10]. Despite being highly accurate, an offline method like EIS can hardly be implemented to investigate a BEV battery's RUL and SoH during the operation [10]–[12]. Therefore, a variety of online methods have been introduced to track the battery's aging while in operation [12]–[14]. The conventional online EIS methods try to create a perturbation signal, for example with the help of a DC-DC power converter around battery's output voltage or battery charger and balancing circuit [5], [12]. However, conducting online EIS normally interferes with the normal operation or needs special equipment, which limits the applicability of these methods [12], [15].

In contrast to conventional battery pack systems with hardwired connections, changing the connections between nearby battery cells/ modules is possible in RBS [16]–[19]. Figure 1 depicts the

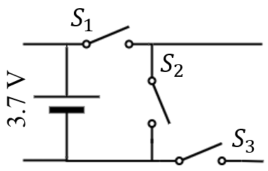

	S_1	S_2	S_3
Bypass	on	off	off
Parallel	on	off	on
Series	off	on	off

Fig. 1: BM3 system with valid switching states [20], [21]

schematic of a Battery Modular Multilevel Management (BM3) Converter System. It consists of a constant voltage source, e.g. a Li-Ion battery, and three semiconductor switches. The three valid switching states for a BM3 module are known as series, parallel, and bypass connection states (Fig. 1). Due to the low battery module/ strand voltages, MOSFETs are commonly used for the discrete switches S_1, S_2, and S_3 [20], [21].
This paper introduces a non-destructive online characterization method based on RBS topologies, in particular BM3 modules or any other RBS enabling parallel switching between neighboring cells. This diagnostic approach needs no additional hardware and does not interfere with the system's normal operation. This method stimulates the battery cell by a balancing current between neighboring cells, that results from parallel switching. Although effective balancing strategies, such as proactive balancing [18], [20], [21], have been proposed to keep the dynamic output voltage and SoC of the cells in RBS at the same level, minor output dynamic-voltage variation is unavoidable. Also, balancing methods like proactive balancing can control the output dynamic-voltage of cells to create the temporary needed Voltage deviation between neighboring cells.

2 Battery Modeling

Direct state monitoring of Li-Ion batteries is not feasible due to the complexity of their internal structure and the aging process. Among all methods for estimating a battery's states like SoH and SoC, model-based methods provide trustworthy and precise estimations of both the SoC and the SoH. Electrochemical/ physics-based models and equivalent circuit models (ECM) are frequently used to characterize Li-Ion batteries due to their accuracy and low level of computational effort [22], [23]. Furthermore, it is feasible to estimate and imitate the battery's behavior, resulting in avoiding cost and time-intensive testing. Figure 2 represents a ECM model. This model consists of a SoC related voltage

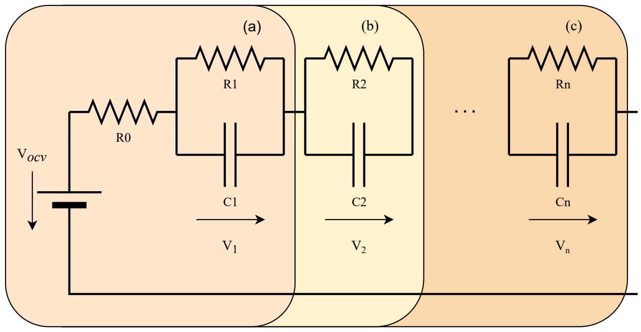

Fig. 2: Most common equivalent circuit model for characterization of vehicle batteries: (a) Thevenin Model ($1RC$), (b) Dual Polarization Model ($2RC$), (c) NRC generalized Thevenin Model [24]

source (V_{ocv}), an internal ohmic resistance R_0 and a number of RC-pairs, which can describe a batteries' voltage-current relation [25]. On the one hand, a higher number of RC-pairs increases the accuracy of modeling, on the other hand, it increases the computational effort drastically. Therefore, the second-order Thevenin model is taken into consideration since it accurately models a batteries' dynamics while keeping simulation times reasonable.

In general, there are two main representations of a second order ECM [24]. Firstly, state space representation, which can be described as follows.

$$V_{\mathrm{t}} = V_{\mathrm{ocv}} - V_1 - V_2 - R_0 I \tag{1}$$

$$V_{\mathrm{t}}\left(t\right) = V_{\mathrm{ocv}} - V_{01} R_1 e^{-\frac{t}{R_1 C_1}} - V_{02} R_2 e^{-\frac{t}{R_2 C_2}} \tag{2}$$

$$\begin{aligned} V_{\mathrm{t}}\left(t\right) = V_{\mathrm{ocv}} - I R_0 - I R_1 [1 - e^{-\frac{t}{R_1 C_1}}] \\ - I R_2 [1 - e^{-\frac{t}{R_2 C_2}}] \end{aligned} \tag{3}$$

$$\frac{dV_1}{dt} = \frac{V_1}{R_1 C_1} + \frac{I}{C_1} \tag{4}$$

$$\frac{dV_2}{dt} = \frac{V_2}{R_2 C_2} + \frac{I}{C_2} \tag{5}$$

Equations (2) and (3) describe the output voltage while relaxation and load, respectively [26], [27]. Secondly, a linear regression model is presented based on bilinear transformation from analog to digital domain Eq. (6).

$$s = \frac{2}{T} \frac{1 - z^{-1}}{1 + z^{-1}} \tag{6}$$

$$E = V_{\mathrm{t}}(s) - V_{\mathrm{ocv}}(s) \tag{7}$$

$$E = -I(s)\left(R_0 + \frac{R_1}{1+R_1C_1s} + \frac{R_2}{1+R_2C_2s}\right) \quad (8)$$

Eqs. (7) and (8) mathematically represent the second order ECM impedance in the s-domain. Equations (9) to (11) are derived by introducing a bilinear transformation into Eq. (8) [28], [29]. The final recursive Eq. (11) needs information from the previous two-time steps. $E(k-1)$ and $E(k-2)$ are the difference between the output voltage and the corresponding open-circuit voltage at the time $k-1$ and $k-2$, respectively. $I(k)$, $I(k-1)$ and $I(k-2)$ represent the current at the time k, $k-1$ and $k-2$, respectively.

$$G(z^{-1}) = \frac{E(k)}{I(k)} \quad (9)$$

$$G(z^{-1}) = \frac{\theta_3 + \theta_4 z^{-1} + \theta_5 z^{-2}}{1 - \theta_1 z^{-1} - \theta_2 z^{-2}} \quad (10)$$

$$E(k) = \theta_1 E(k-1) + \theta_2 E(k-2) + \theta_3 I + \theta_4 I(k-1) + \theta_5 I(k-2) \quad (11)$$

To simplify Eq. (11), the variables a,b,c,d,f are defined as follows.

$$a = R_0 \quad (12)$$

$$b = R_1C_1R_2C_2 \quad (13)$$

$$c = R_1C_1 + R_2C_2 \quad (14)$$

$$d = R_0 + R_1 + R_2 \quad (15)$$

$$f = R_0R_1C_1 + R_0R_2C_2 + R_2R_1C_1 + R_1R_2C_2 \quad (16)$$

The coefficients of Eq. (11) can be re-written with respect to a,b,c,d,f as follows.

$$\theta_1 = \frac{8b - 2T^2}{4b + 2cb + T^2} \quad (17)$$

$$\theta_2 = \frac{4cT}{4b + 2cb + T^2} - 1 \quad (18)$$

$$\theta_3 = -\frac{4ab - 2fT + dT^2}{4b + 2cb + T^2} \quad (19)$$

$$\theta_4 = \frac{8ab - 2dT^2}{4b + 2cb + T^2} \quad (20)$$

$$\theta_5 = -\frac{4ab - 2ft + dT^2}{4b + 2cb + T^2} \quad (21)$$

Based on the battery's prior states, linear recursive Eq. (11) and its simplified coefficient, Eqs. (12) to (16), can be used to determine the battery's dynamic output voltage. However, the time-varying parameters of the battery must be calculable at any given time. As a result, R_0, R_1, C_1, R_2 and C_2 must be derived from θ_1, θ_2, θ_3, θ_4, θ_5 (Eqs. (22) to (35)).

$$a = \frac{(\theta_4 - \theta_3 - \theta_5)}{(1 + \theta_1 - \theta_2)} \quad (22)$$

$$b = \frac{T^2(1 + \theta_1 - \theta_2)}{(1 - \theta_1 - \theta_2)} \quad (23)$$

$$c = \frac{T(1 + \theta_2)}{(1 - \theta_1 - \theta_2)} \quad (24)$$

$$d = \frac{(-\theta_4 - \theta_3 - \theta_5)}{(1 - \theta_1 - \theta_2)} \quad (25)$$

$$f = \frac{T(\theta_5 - \theta_3)}{(1 - \theta_1 - \theta_2)} \quad (26)$$

$$R_1C_1 = \tau_1 \quad (27)$$

$$R_2C_2 = \tau_2 \quad (28)$$

$$b = \tau_1 + \tau_2 \quad (29)$$

$$c = \tau_1\tau_2 \quad (30)$$

$$R_0 = a \quad (31)$$

$$R_1 = \frac{\tau_1(d - a) + ac - f}{\tau_1 - \tau_2} \quad (32)$$

$$R_2 = d - a - R_1 \quad (33)$$

$$C_1 = \frac{\tau_1}{R_1} \quad (34)$$

$$C_2 = \frac{\tau_2}{R_2} \quad (35)$$

3 Simulation and Proof of Concept

A BM3 converter system is implemented in MATLAB/SIMULINK to demonstrate the concept's validity. For simplicity, only two cells are implemented. The internal resistances of all switches (MOSFETs) are assumed as negligible. However, real switches with non-negligible internal resistance can only cause a voltage offset in the measured voltage and can easily be subtracted from the voltage measurement.

As part of the simulation, two battery cells based on second order ECM are created and tuned according to the test result of a 'LG18650HG2' and 'LG18650MJ1' battery cell. The cell models are initialized with 90 % and 95 % SoC, respectively, which leads to a 0.05 V voltage deviation between the cells. The two cells are switched in parallel for 0.3 s. Subsequently, the cells' relaxation periods are monitored for 2.6 s. Figure 3 represents the

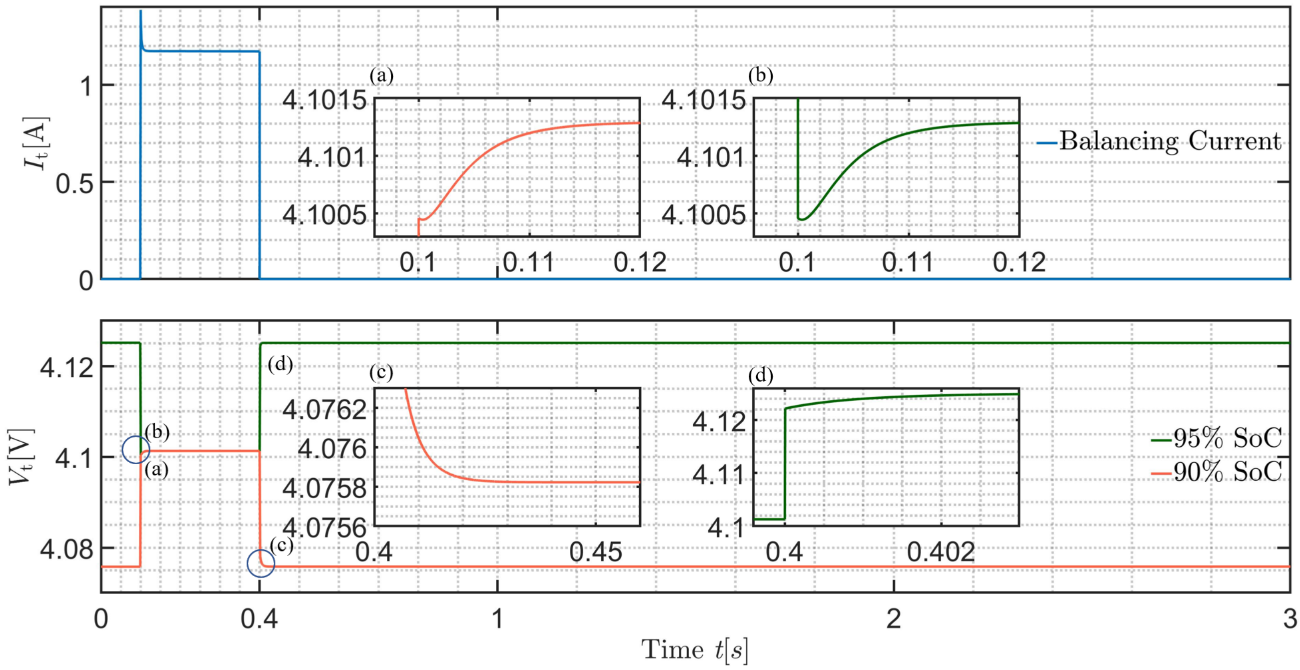

Fig. 3: Monitored cell current and voltage of cells during parallel switching and relaxation. (a) Dynamic output voltage of the cell with lower SoC during balancing. (b) Dynamic output voltage of the cell with higher SoC during balancing. (c) Dynamic output voltage of the cell with lower SoC during relaxation. (d) Dynamic output voltage of the cell with higher SoC during relaxation.

balancing current and dynamic output voltage of corresponding cells. The balancing current consists of a short current peak followed by a near constant current phase. The current peak magnitude depends on the initial voltage deviation and sum of ohmic resistances (R_0) of the corresponding cells, therefore, it is important to keep the cells' dynamic output voltages as close as possible while parallel switching to avoid high current peaks. As can be seen in Fig. 3 (a) and (b), the cells' output voltage are the same during balancing and this behavior is highly dynamic as it is determined not only by the internal structure of one cell but also by both corresponding cells during balancing. As mentioned above, assuming that the switches' internal resistance is negligible, the cell's output voltage is without any offset.

Since both cells have the same output voltage while balancing, it is not possible to distinguish the individual behavior and the corresponding internal structure just by looking at the balancing part. Alternatively, the relaxation part of each cell depends only on its internal structure. However, this part is not directly determined by the input current. Therefore, it is important to examine the relaxation part, Fig. 3 (c) and (d), as supplementary information to characterize each individual cell.

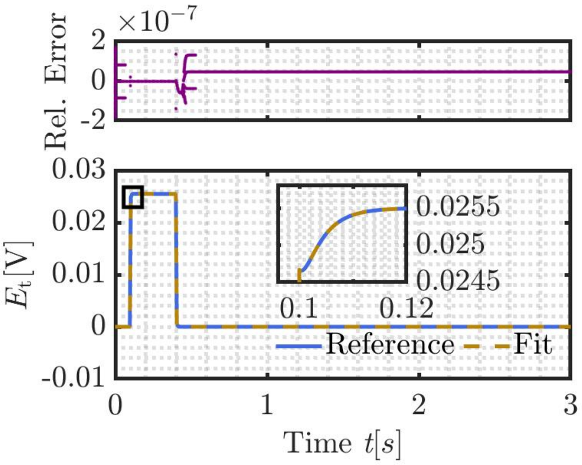

Fig. 4: Battery modeling based on 2nd order ECM and Pulse characterization(fitting) based on 2nd order ECM and its relative error.

3.1 Characterization

Within the scope of this paper, the linear recursive Eq. (11) and its simplified coefficient, Eqs. (12) to (16), are used to characterize and model the dynamic output voltage of each cell.

Figure 4 represents the quality of pulse fitting and

$R_0[m\Omega]$	$R_1[m\Omega]$	$C_1[F]$	$R_2[m\Omega]$	$C_2[mF]$
17.80	1.30	1.087	1.20	563.0
17.81	1.31	1.086	1.18	562.9

Tab. 1: Tuned (first row) and estimated (second row) dynamic parameters of the battery cell.

characterization and its relative error. Thanks to the linear recursive, Eq. (11), and based on the 'lsqcurvefit/MATLAB' algorithm, highly accurate characterization with relative error in the range of 10^{-7} is possible. Finally, the dynamic parameters of each cell can be estimated based on Eqs. (31) to (35). Table 1 shows the tuned and estimated dynamic parameters of the cell with higher SoC before balancing.

Contrary to reality and for the purpose of simplicity, the second order ECM is used to simulate the cell's behavior while balancing. However, as discussed above, the higher the number of RC elements, the higher the modeling accuracy. Thus, the real cell can be viewed as an ECM with an infinite number of RC elements or NRC. On the other hand, the real cell model (NRC model) generates highly detailed and complex data that cannot be fully captured by a simple 2nd order ECM.

For the simulation and characterization of more complex data (real cell), the battery model used is upgraded with a third RC element. Then, the generated information is characterized with simple second order ECM. Figure 5 shows the slight reduction in fitting accuracy, namely increasing the relative error from $2 \times 10^{-}7$ to $5 \times 10^{-}5$, but the behavior of the cell is still modeled to a large extent. As expected, the estimated dynamic parameters are not the same as for the tuned model, since the behavior of three RC is modeled by two RC. However, these two models ($2RC$ and $3RC$) have the same output voltage feedback with respect to the balancing current as Eq. (36).

$$E_{2\mathrm{RC}}(s) \simeq E_{3\mathrm{RC}}(s) \tag{36}$$

By solving Eq. (36) in the charge and relaxation condition based on Eqs. (2) and (3) and assuming that the different time constants (τ) of the battery do not differ too much, The following equations can be obtained after simplification.

$$\ln \frac{(\sum_0^2 R_i)(\prod_1^2 R_i)}{(\sum_0^n R_j)(\prod_1^n R_j)} = T(\sum_1^2 \frac{1}{\tau_i} - \sum_1^n \frac{1}{\tau_j}) \tag{37}$$

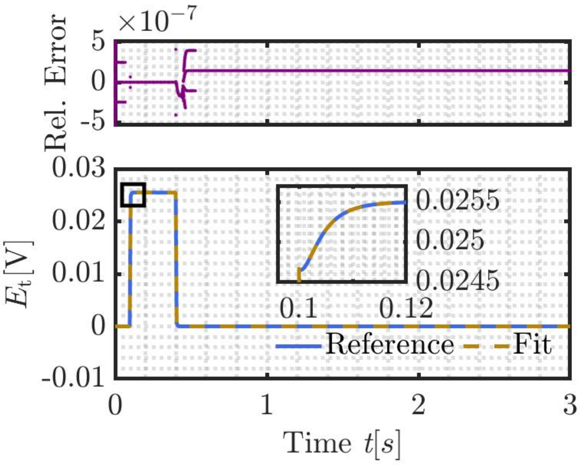

Fig. 5: Battery modeling based on the second order ECM and Pulse characterization (fitting) based on the third order ECM and its relative error.

$R_0[m\Omega]$	$R_1[m\Omega]$	$R_2[m\Omega]$	$R_3[m\Omega]$	$\sum[m\Omega]$
17.80	1.190	1.320	1.42	21.740
17.81	2.647	1.282	–	21.739

Tab. 2: Tuned (first row) and estimated (second row) internal resistances of the battery cell.

$$\ln \frac{(\prod_1^2 R_i)}{(\prod_1^n R_j)} = T(\sum_1^2 \frac{1}{\tau_i} - \sum_1^n \frac{1}{\tau_j}) \tag{38}$$

From the equality of the Eqs. (37) and (38), it follows that the sum of the internal resistances of two ECM with a different number of RC elements that have the same voltage response to the specific current input is equal, Eq. (39) and table 2. Therefore, the sum of internal resistances of the modeled ECM can be a practical value to track and estimate the SoH of each cell. Resistance dependent SoH or $\mathrm{SoH_r}$ is normally defined as the ratio between the actual resistance (R_{act}) and the battery's beginning of life's resistance (R_{BoL}). In the context of this paper, a new parameter, $\mathrm{SoH_{sor}}$ or sum of resistances dependent SoH, is introduced. Equation (40) represents the $\mathrm{SoH_{sor}}$ as a ratio between the sum of actual battery's resistances and the sum of battery's beginning of life's resistances.

$$\sum_0^n R_i \simeq \sum_0^m R_j \tag{39}$$

$$SoH_{sor} = \frac{(\sum_0^n R_i)_{act}}{(\sum_0^n R_i)_{BoL}} \tag{40}$$

4 Conclusion

The proposed online characterization method based on the recursive derivation of parameters in the time domain can accurately estimate the sum of the battery's resistances. Also, the new parameter, $\mathrm{SoH}_{\mathrm{sor}}$, is introduced to track the battery's aging phenomena dependent on the sum of the battery's resistances. In addition, the proposed approach does not disrupt the normal operation of the battery system and can be implemented in any RBS with the ability to connect adjacent cells in parallel.

References

[1] J. Buberger, A. Kersten, M. Kuder, R. Eckerle, T. Weyh, and T. Thiringer, "Total co2-equivalent life-cycle emissions from commercially available passenger cars," *Renewable and Sustainable Energy Reviews*, vol. 159, p. 112 158, 2022.

[2] H. H. Abdeltawab and Y. A.-R. I. Mohamed, "Market-oriented energy management of a hybrid wind-battery energy storage system via model predictive control with constraint optimizer," *IEEE Transactions on Industrial Electronics*, vol. 62, no. 11, pp. 6658–6670, 2015. DOI: 10.1109/TIE.2015.2435694.

[3] S. Vazquez, S. M. Lukic, E. Galvan, L. G. Franquelo, and J. M. Carrasco, "Energy storage systems for transport and grid applications," *IEEE Transactions on Industrial Electronics*, vol. 57, no. 12, pp. 3881–3895, 2010. DOI: 10.1109/TIE.2010.2076414.

[4] D. Velasco de la Fuente, C. L. Trujillo Rodríguez, G. Garcerá, E. Figueres, and R. Ortega Gonzalez, "Photovoltaic power system with battery backup with grid-connection and islanded operation capabilities," *IEEE Transactions on Industrial Electronics*, vol. 60, no. 4, pp. 1571–1581, 2013. DOI: 10.1109/TIE.2012.2196011.

[5] S. M. R. Islam and S.-Y. Park, "Precise online electrochemical impedance spectroscopy strategies for li-ion batteries," *IEEE Transactions on Industry Applications*, vol. 56, no. 2, pp. 1661–1669, 2020. DOI: 10.1109/TIA.2019.2958555.

[6] C. Pastor-Fernández, W. Dhammika Widanage, J. Marco, M.- Gama-Valdez, and G. H. Chouchelamane, "Identification and quantification of ageing mechanisms in lithium-ion batteries using the eis technique," in *2016 IEEE Transportation Electrification Conference and Expo (ITEC)*, 2016, pp. 1–6. DOI: 10.1109/ITEC.2016.7520198.

[7] N. Meddings, M. Heinrich, F. Overney, J.-S. Lee, V. Ruiz, *et al.*, "Application of electrochemical impedance spectroscopy to commercial li-ion cells: A review," *Journal of Power Sources*, vol. 480, p. 228 742, 2020. DOI: https://doi.org/10.1016/j.jpowsour.2020.228742.

[8] S. Müller and P. Massarani, "Transfer-function measurement with sweeps," *Journal of the Audio Engineering Society*, vol. 49, Jun. 2001.

[9] A. Barai, K. Uddin, M. Dubarry, L. Somerville, A. McGordon, *et al.*, "A comparison of methodologies for the non-invasive characterisation of commercial li-ion cells," *Progress in Energy and Combustion Science*, vol. 72, pp. 1–31, 2019. DOI: https://doi.org/10.1016/j.pecs.2019.01.001.

[10] J. Li, C. Arbizzani, S. Kjelstrup, J. Xiao, Y. yao Xia, *et al.*, "Good practice guide for papers on batteries for the journal of power sources," *Journal of Power Sources*, vol. 452, p. 227 824, 2020. DOI: https://doi.org/10.1016/j.jpowsour.2020.227824.

[11] W. Li, Q.-A. Huang, C. Yang, J. Chen, Z. Tang, *et al.*, "A fast measurement of warburg-like impedance spectra with morlet wavelet transform for electrochemical energy devices," *Electrochimica Acta*, vol. 322, p. 134 760, 2019. DOI: https://doi.org/10.1016/j.electacta.2019.134760.

[12] J. A. A. Qahouq and Z. Xia, "Single-perturbation-cycle online battery impedance spectrum measurement method with closed-loop control of power converter," *IEEE Transactions on Industrial Electronics*, vol. 64, no. 9, pp. 7019–7029, 2017. DOI: 10.1109/TIE.2017.2686324.

[13] M. Abedi Varnosfaderani and D. Strickland, "A comparison of online electrochemical spectroscopy impedance estimation of batteries,"

IEEE Access, vol. 6, pp. 23 668–23 677, 2018. DOI: 10.1109/ACCESS.2018.2808412.

[14] A. Kersten, M. Kuder, W. Han, T. Thiringer, A. Lesnicar, *et al.*, "Online and on-board battery impedance estimation of battery cells, modules or packs in a reconfigurable battery system or multilevel inverter," in *IECON 2020 The 46th Annual Conference of the IEEE Industrial Electronics Society*, 2020, pp. 1884–1891. DOI: 10.1109/IECON43393.2020.9254515.

[15] J. Zhu, Z. Sun, X. Wei, and H. Dai, "A new lithium-ion battery internal temperature on-line estimate method based on electrochemical impedance spectroscopy measurement," *Journal of Power Sources*, vol. 274, pp. 990–1004, 2015. DOI: https://doi.org/10.1016/j.jpowsour.2014.10.182.

[16] S. Ci, N. Lin, and D. Wu, "Reconfigurable battery techniques and systems: A survey," *IEEE Access*, vol. 4, pp. 1175–1189, 2016. DOI: 10.1109/ACCESS.2016.2545338.

[17] F. Chen, W. Qiao, and L. Qu, "A modular and reconfigurable battery system," in *2017 IEEE Applied Power Electronics Conference and Exposition (APEC)*, 2017, pp. 2131–2135. DOI: 10.1109/APEC.2017.7930993.

[18] W. Han, T. Wik, A. Kersten, G. Dong, and C. Zou, "Next-generation battery management systems: Dynamic reconfiguration," *IEEE Industrial Electronics Magazine*, vol. 14, no. 4, pp. 20–31, 2020. DOI: 10.1109/MIE.2020.3002486.

[19] A. Lesnicar and R. Marquardt, "An innovative modular multilevel converter topology suitable for a wide power range," in *2003 IEEE Bologna Power Tech Conference Proceedings,*, vol. 3, 2003, 6 pp. Vol.3–. DOI: 10.1109/PTC.2003.1304403.

[20] M. Kuder, J. Schneider, A. Kersten, T. Thiringer, R. Eckerle, and T. Weyh, "Battery modular multilevel management (bm3) converter applied at battery cell level for electric vehicles and energy storages," in *PCIM Europe digital days 2020; International Exhibition and Conference for Power Electronics, Intelligent Motion, Renewable Energy and Energy Management*, 2020, pp. 1–8.

[21] A. Mashayekh, A. Kersten, M. Kuder, J. Estaller, M. Khorasani, *et al.*, "Proactive soc balancing strategy for battery modular multilevel management (bm3) converter systems and reconfigurable batteries," in *2021 23rd European Conference on Power Electronics and Applications (EPE'21 ECCE Europe)*, 2021, P.1–P.10.

[22] Z. Geng, S. Wang, M. J. Lacey, D. Brandell, and T. Thiringer, "Bridging physics-based and equivalent circuit models for lithium-ion batteries," *Electrochimica Acta*, vol. 372, p. 137 829, 2021.

[23] J. Estaller, A. Kersten, M. Kuder, A. Mashayekh, J. Buberger, *et al.*, "Battery impedance modeling and comprehensive comparisons of state-of-the-art cylindrical 18650 battery cells considering cells' price, impedance, specific energy and c-rate," in *2021 IEEE International Conference on Environment and Electrical Engineering and 2021 IEEE Industrial and Commercial Power Systems Europe (EEEIC / I CPS Europe)*, 2021, pp. 1–8.

[24] L. Komsiyska, T. Buchberger, S. Diehl, M. Ehrensberger, C. Hanzl, *et al.*, "Critical review of intelligent battery systems: Challenges, implementation, and potential for electric vehicles," *Energies*, vol. 14, p. 5989, Sep. 2021. DOI: 10.3390/en14185989.

[25] O. Theliander, A. Kersten, M. Kuder, W. Han, E. A. Grunditz, and T. Thiringer, "Battery modeling and parameter extraction for drive cycle loss evaluation of a modular battery system for vehicles based on a cascaded h-bridge multilevel inverter," *IEEE Transactions on Industry Applications*, vol. 56, no. 6, pp. 6968–6977, 2020. DOI: 10.1109/TIA.2020.3026662.

[26] D. Liu, X. Wang, M. Zhang, and M. Gong, "Soc estimation of lithium battery based on n-2rc model in electric vehicle," in *2019 Chinese Control And Decision Conference (CCDC)*, 2019, pp. 2916–2921. DOI: 10.1109/CCDC.2019.8833008.

[27] B. Fridholm, M. Nilsson, and T. Wik, "Robustness comparison of battery state of charge observers for automotive applications," *IFAC*

Proceedings Volumes (IFAC-PapersOnline), vol. 19, pp. 2138–2146, Jan. 2014.

[28] X. Sun, J. Ji, B. Ren, C. Xie, and D. Yan, "Adaptive forgetting factor recursive least square algorithm for online identification of equivalent circuit model parameters of a lithium-ion battery," *Energies*, vol. 12, p. 2242, Jun. 2019. DOI: 10.3390/en12122242.

[29] B. Xia, R. Huang, Z. Lao, R. Zhang, Y. Lai, *et al.*, "Online parameter identification of lithium-ion batteries using a novel multiple forgetting factor recursive least square algorithm," *Energies*, vol. 11, p. 3180, Nov. 2018. DOI: 10.3390/en11113180.